Check for updates

Controllable and directional growth of Er:Lu₂O₃ single crystals by the edge-defined film-fed technique

Yanru Yin, Guiji Wang, Zhitai Jia, [iD] * Wenxiang Mu, Xiuwei Fu, Jian Zhang and Xutang Tao [iD] *

The sesquioxide Lu₂O₃ single crystal has enormous potential applications as host material for solid-state lasers operating at high average powers, and its development is limited by the lack of large sized single crystals with high quality. Compared with the traditional Czochralski (Cz) method, the edge-defined film-fed growth (EFG) method, employing a die or a shaper, doesn't make the grown crystal come into contact with the melt in crucible directly during the growth process. Therefore, the growth interface is stable and the serious bottleneck problems of a "w"-shaped isotherm in the Czochralski method could be avoided effectively. Herein, the EFG method may be a promising technique to obtain ultra-high temperature sesquioxide single crystals with a large size, and more importantly, high quality. Accordingly, the sesquioxide Lu₂O₃ single crystal has been grown controllably with an oriented seed by the EFG method for the first time and the EFG method is promoted to an extremely high temperature of 2450 °C. The dimensions of the grown crystal are Φ 25 × 30 mm³, and the difficulties encountered during the crystal growth have been discussed in detail. Furthermore, the quality of the crystal has been evaluated. The optical properties of the grown crystal have been investigated.

1. Introduction

A high average power solid-state laser with high operating efficiency is desired, especially for applications in industrial processing, medical treatment, environmental monitoring and scientific research. Desirable host crystals for solid state lasers should possess a high thermal conductivity. From this point of view, the rare-earth sesquioxide Lu₂O₃ could be a very promising laser host material. The thermal conductivity of undoped Lu₂O₃ is as high as 12.8 W m⁻¹ K⁻¹, and more importantly, it remains nearly constant under heavy rare-earth ion doping.[1] On the other hand, the maximum phonon energy of Lu₂O₃ is 618 cm⁻¹,[2] which is lower than that of YAG (857 cm⁻¹).[3] Lu₂O₃ exhibits a wide spectral transparency in the range of 0.2–8 μm and possesses comparably low maximum phonon energies, making it a suitable laser host material for lasers up to the mid-infrared spectral range without the risk of strong non-radiative phononic de-excitation.[4,5] Therefore, Lu₂O₃, with high Er³⁺ doping concentrations, is an ideal host material for 3 μm lasers.[6–8]

Lu₂O₃ crystals have been so far grown by the Verneuil technique,[9] the flux method,[10] the floating zone technique,[11] the laser heated pedestal growth,[12] the hydrothermal

technique,[13–15] the micro pull down method,[16] and the heat exchanger method.[17] Recently, the need for large sized and high quality Lu₂O₃ crystals has been increasing for high power laser generation. The Czochralski (Cz) method is one of the most important techniques for growing large sized single crystals. However, the melting point of Lu₂O₃, 2450 °C, is extremely high, which makes it very difficult to grow single crystals by the Cz method.[18] Firstly, it is rather difficult to find suitable crucible materials for such high growth temperature. Secondly, a "w"-shaped isotherm at the crystal–melt interface caused by very high radiation losses at the free melt surface makes the length of the growing crystals always limited to about 6 mm.

The edge-defined film-fed growth (EFG) method is another highly efficient bulk crystal growth method, and has been widely used in the crystal growth of Si, sapphire, Nd:YVO₄, Ga₂O₃, *etc.*[19–27] The EFG method, evolved from the CZ method, employs a die or a shaper placed in the crucible. Compared with that from the traditional Cz method, the grown crystal doesn't make contact with the melt in crucible directly during the growth process. The melt is transported from the crucible to the shaped top surface of the die by a narrow slit or channel due to capillary forces, which can avoid mostly the influence of melt convection in the crucible. As a result, the growth interface is more stable and the problem of the "w"-shaped isotherm in the Czochralski

State Key Laboratory of Crystal Materials, Shandong University, Jinan, Shandong 250100, China. E-mail: z.jia@sdu.edu.cn, txt@sdu.edu.cn

method could be avoided effectively. In consequence, the EFG method may be a promising technique to obtain ultra-high temperature sesquioxide single crystals with a large size and, more importantly, high quality.

In this work, a bulk sesquioxide Lu_2O_3 single crystal with Er^{3+} doping has been grown with an oriented seed using the EFG technique for the first time. By designing the Re die surface shape and position, after-heater height, and size of thermal insulation materials, the instability of the solid–liquid interface and the serious bottleneck problems of the "w"-shaped isotherm during the process of crystal growth were successfully overcome. The dimensions of the grown crystal are $\Phi\ 25 \times 30\ mm^3$. The difficulties encountered during the crystal growth have been thoroughly discussed. The quality of the crystal has been evaluated. Furthermore, the optical properties of the grown crystal have been investigated.

2. Experimental section

2.1 Crystal growth

The $Er:Lu_2O_3$ single crystals were grown in a modified EFG furnace with a rhenium crucible of 60 mm as well as a rhenium die of 25 mm in diameter, under a slightly reducing $Ar + H_2$ atmosphere. Raw powder materials, 99.99% pure Lu_2O_3 and Er_2O_3, were accurately weighed. After mixing adequately, the mixture was pressed into tablets to fill the crucible. A small piece of undoped Lu_2O_3 crystal with the <541> direction, obtained by the HEM, was employed as the seed. The pulling rate was set to be 0.5 mm h^{-1}. After the growth, the crystal was cooled down to room temperature at a rate of 50–55 °C h^{-1}. The as-grown $Er:Lu_2O_3$ crystals were annealed at 1650 °C for 15 h in air in order to eliminate the oxygen vacancies and release the thermal stress formed during the growth.[28–31] Finally, an $Er:Lu_2O_3$ single crystal with dimensions of $\Phi\ 25 \times 30\ mm^3$ was grown successfully, as shown in Fig. 1.
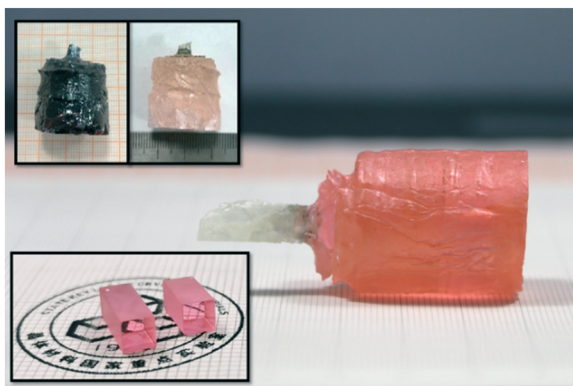

Fig. 1 Photographs of the grown $Er:Lu_2O_3$ crystal boule. The inserts, in the upper left corner, show the $Er:Lu_2O_3$ boule before (left) and after (right) post-growth annealing. The insert, in the lower left corner, shows the photograph of end polished rods of the grown $Er:Lu_2O_3$ crystal.

2.2 Characterization techniques

The crystallinity of the grown crystal was characterized with high-resolution X-ray diffraction (HRXRD) on a plate of one millimeter thickness using a Bruker D8 Discovery system equipped with a four-circle monochromator set for Cu $K\alpha_1$ radiation (λ = 1.54056 Å). The optical homogeneity was identified using a ZYGO GPI XP/D optical interferometer equipped with a He–Ne laser (λ = 632.8 nm). A crystal slice was cut and processed in a wedge angle ($\sim$15′). Two surfaces were polished well to avoid the light scattering and wave distortion. ZYGO MetroPro software was used to record and analyze the results. X-ray Laue back-reflection measurements were carried out using a real-time back-reflection Laue camera system (Multiwire MWL 120 with Northstar software) to further assess the crystalline perfection. An $Er:Lu_2O_3$ slice with dimensions of $\Phi\ 25 \times 1\ mm^3$ was employed for the measurement. The transmittance spectrum was measured with a HITACHI U-4100 spectrophotometer in the UV-vis-near IR range (200–2500 nm with a resolution of 1 nm) and with a PerkinElmer Spectrum 100 FT-IR spectrometer in the middle IR region (2500–10 000 nm with a resolution of 4 cm^{-1}). A 2.1 mm thick plate was used for this measurement.

3. Results and discussion

3.1 Crystal growth

In the initial growth, several key issues for $Er:Lu_2O_3$ crystal growth were needed to be clarified, such as the selection of crucible materials, the structure design of thermal insulation materials, and the optimization of seeds. The discussions are as follows:

(i) The usage of crucible materials was extremely limited by the high melting point of Lu_2O_3. The crucible materials must withstand high growth temperature as well as possess good chemical stability to the melt and the surrounding thermal insulation. A tungsten crucible was tested at the beginning because of its low cost, but it reacted with the raw material violently before the melting point. No improvements were found as the H_2 concentration increased. Finally, we found a rhenium crucible that can satisfy the specific requirements of crystal growth, although it was still slightly corroded by the Lu_2O_3 melt.

(ii) Concerning the extremely high melting point of Lu_2O_3 (2450 °C) and easily oxidizable characteristic of the rhenium crucible, we tested graphite cylinders and felt for thermal insulation. However, the melt was seriously polluted by the graphite, and the black colour of the crystal can't be eliminated by annealing in air. So, we changed them to zirconia cylinders and fibres. In addition, the distance between the crucible and zirconia must be kept beyond 20 mm to prevent the melting of the zirconia bricks. More importantly, the zirconia thermal insulation must be thick enough to decrease the heat dissipation, otherwise the crucible will be overheated to be spiny, or even be melted, while the raw materials cannot be melted totally.

(iii) A transparent Lu_2O_3 ceramic rod was employed as the seed for the first trial, but it turned black and was seriously melted before the melt being transported through the slits to the top of the die. Then, Lu_2O_3 crystals (Fig. 2) obtained by the HEM were used, and we could seed successfully. We supposed that a small amount of impurities remaining in the ceramic significantly reduces the melting point of the material.

(iv) Instead of being a cylinder, the crystal was spiral (Fig. 3a), or shaped like a trumpet after seeding (Fig. 3b). This might be related to the instability of the melt surface caused by the concave solid–liquid interface. At very high temperatures, the heat of the surface of the die was lost by means of radiation mostly. The heat in the interface region of the growing crystal dissipated mainly by means of heat conduction. So, the temperature near the interface was higher than that at the uncovered surface of the melt on the die. When the spiral or trumpet-shaped growth appeared, the crystal separated from the melt despite strong cooling, so the growth needed to be interrupted. These problems were successfully solved by designing a rhenium after-heater device and improving the design of the Re die surface shape and position. The after-heater was a rhenium cylinder with a diameter of 60 mm, a height of 40 mm, and a thickness of 1.5 mm. By putting the after-heater on the crucible, the temperature of the upper hot zone was raised, the longitudinal temperature gradient was reduced accordingly, and the temperature field of the surface of the die became more uniform. In the end, the instability of the solid–liquid interface and the serious bottleneck problems of the "w"-shaped isotherm during the process of crystal growth were successfully overcome.

3.2 Chemical composition and segregation coefficient

An Agilent 5110 ICP-OES was used to measure the concentrations of Er and Lu in the crystal. The measured sample was cut from the top of the grown crystal and dissolved in a mixture of sulfuric and phosphoric acid. The ICP result showed that the concentration of Er was 7.83 at%. The effective segregation coefficient k_{eff} can be calculated by the following equation:[32]

Fig. 2 Lu_2O_3 crystal seeds with the <541> direction obtained by the HEM.

Fig. 3 Photographs of (a) spiral and (b) trumpet-shaped crystals grown by the EFG method.

$$k_{eff} = C_s/C_l$$

where C_s and C_l are the doping concentrations of the ions in the crystal and the melt. According to the measured result and the concentration of starting materials, the effective segregation coefficient of Er^{3+} in the Er:Lu_2O_3 crystal grown by the EFG method was calculated to be 0.92. The value is close to the ideal value of 1.0, which means that Er^{3+} was distributed homogeneously in the EFG Er:Lu_2O_3 crystal.

Trace rhenium was detected by ICP with a concentration of 52.44 ppm. The concentration of impurity Re is much lower than that in the Lu_2O_3 crystal grown by the HEM from a Re-crucible, where the microscopic visible Re-inclusions vary between 5 and 20 μm in size.[33] In addition, we found lots of Re-floats accumulated on the surface of the melt, attached to the crucible. So, we supposed that the lower concentration of Re may be attributed to the capillary force generated in the EFG method, which could transfer the melt from the bottom of the crucible to the top surface of the die through a narrow slit, thereby keeping most of the Re-floats away from being sucked to the growth interface. In
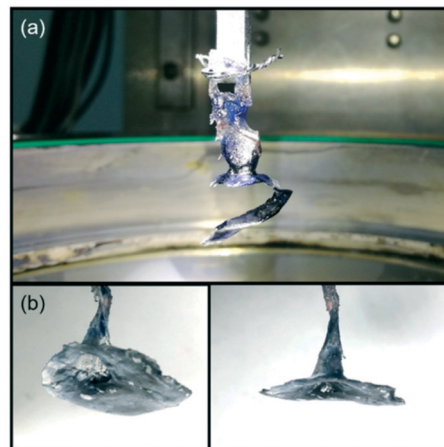

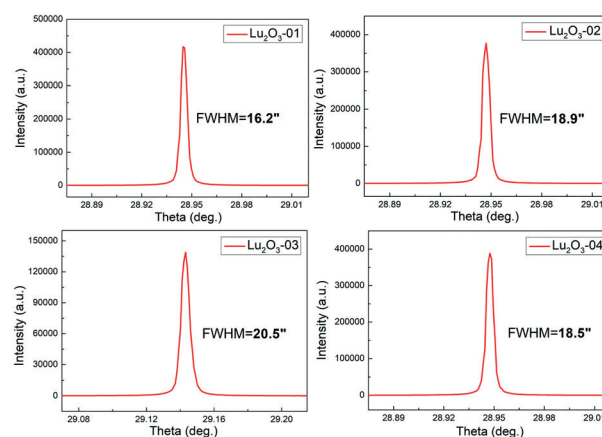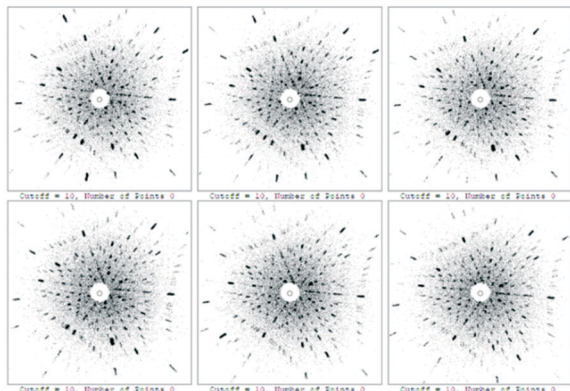**Fig. 4** Rocking curves of the Er:Lu_2O_3 crystal.

Fig. 5 Characteristic Laue back-reflection patterns at different positions.

consequence, the concentration of impurity Re was significantly reduced.

3.3 Crystal quality

The quality of the grown $Er:Lu_2O_3$ was characterized by HRXRD and Laue back-reflection measurements. Test points were taken from different parts of the sample. All the peaks of the rocking curves were symmetrical. The typical full widths at half maximum (FWHM) were as small as 16.2, 18.9, 20.5 and 18.5 arcsec, respectively, as shown in Fig. 4. Laue back-reflection measurements were broadly applied to investigate the crystallinity and orientation of an as-grown crystal. As can be apparently seen from Fig. 5, the characteristic Laue back-reflection patterns at different positions along the crystal were uniform, clear, and bright. And there was no obvious splitting of the diffraction spots. The above results indicated the good crystalline quality of the $Er:Lu_2O_3$ crystal grown by the EFG method.

An important property of an optical component is the homogeneity of the refractive index of the material from which it is made. Variations in the material's refractive index will affect the wavefront passing through it. The optical homogeneity of the $Er:Lu_2O_3$ crystal was determined using a ZYGO GPI optical interferometer. A wafer with dimensions of
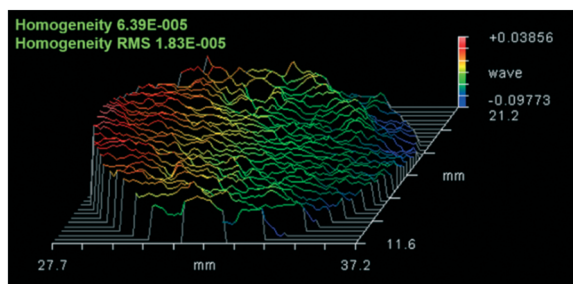

Fig. 6 Optical homogeneity in realistic fixed 3D views of the $Er:Lu_2O_3$ single crystal, which shows the wavefront variations in 3D views. The unit of the 3D views of the measurement results is wavelength (λ = 632.8 nm), representing the relative change of the refractive index at different positions.
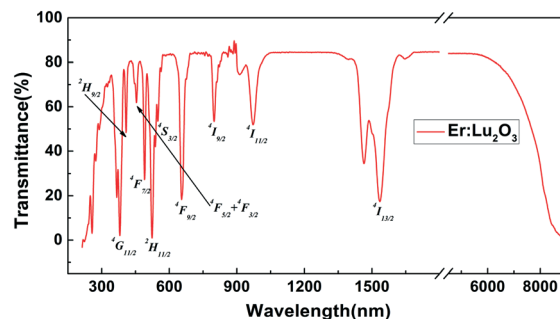

Fig. 7 Transmittance spectrum of the 2.1 mm thick uncoated $Er:Lu_2O_3$ single crystal sample.

Φ 10 × 1.4 mm^3 was cut and polished from the bulk crystal. Fig. 6 shows the result of the optical homogeneity measurement in realistic fixed 3D views. The value of the homogeneity was determined to be 6.39×10^{-5}, indicating that the grown crystal had good optical homogeneity.

3.4 Transmittance

The transmittance spectrum of the $Er:Lu_2O_3$ single crystal sample with a thickness of 2.1 mm is shown in Fig. 7, which shows a high optical transparency (>80%) from 430 nm to 6300 nm. The characteristic absorption bands of Er^{3+} centered at around 382, 408, 454, 490, 523, 549, 655, 799, 972, and 1535 nm could be observed, and correspond to the transitions from ground state $^4I_{15/2}$ to excited states $^4G_{11/2}$, $^2H_{9/2}$, $^4F_{5/2} + ^4F_{3/2}$, $^4F_{7/2}$, $^2H_{11/2}$, $^4S_{3/2}$, $^4F_{9/2}$, $^4I_{9/2}$, $^4I_{11/2}$, and $^4I_{13/2}$, respectively. The absorption bands of $Er:Lu_2O_3$ in the present study were also consistent with those reported from materials grown by the hydrothermal method.[13] Furthermore, the IR absorption cutoff wavelength was 8.7 μm. Therefore, the Lu_2O_3 single crystal grown by the EFG method exhibited a wide transparent region (0.23–8.7 μm), which was very beneficial to optical applications.

Conclusions

In conclusion, through continuous improvement of the experimental technology and scheme, we have used the EFG method to grow an $Er:Lu_2O_3$ single crystal with an ultra-high melting point and excellent laser performance for the first time. Bulk Er^{3+} doped Lu_2O_3 has been grown with a rhenium crucible and die by the EFG method. The dimensions of the grown crystal are as large as Φ 25 × 30 mm^3 with the current technical solutions and setups. The growth issues, such as the selection of crucible materials, the structure design of thermal insulation materials, and the optimization of seeds, have been discussed in detail. Furthermore, the peaks of the X-ray rocking curves are symmetrical. The FWHM values are as small as 16.2, 18.9, 20.5 and 18.5 arcsec, respectively, indicating the good crystalline quality of the grown $Er:Lu_2O_3$ crystal. The grown crystal has good optical homogeneity with a value of 6.39×10^{-5}. We believe that this work opens up a brand-new way for growing high-quality bulk Lu_2O_3 crystals

controllably and directionally. Of course, through the research of enlarged process technology, Lu$_2$O$_3$ crystals of a larger size can also be obtained by this way in the future.

Conflicts of interest

There are no conflicts of interest to declare.

Acknowledgements

Notes and references

1 R. Peters, C. Kränkel, S. T. Fredrich-Thornton, K. Beil, K. Petermann, G. Huber, O. H. Heckl, C. R. E. Baer, C. J. Saraceno, T. Südmeyer and U. Keller, *Appl. Phys. B: Lasers Opt.*, 2011, **102**, 509–514.

2 E. Mix, *Ph.D. dissertation*, Univ. Hamburg, Hamburg, Germany, 1999.

3 J. P. Hurell, S. P. S. Porto, I. F. Chang, S. S. Mitra and R. P. Baumann, *Phys. Rev.*, 1968, **173**, 851–856.

4 L. Fornasiero, *Ph.D. dissertation*, Univ. Hamburg, Hamburg, Germany, 1999.

5 C. Kränkel, *IEEE J. Sel. Top. Quantum Electron.*, 2015, **21**, 1602013.

6 T. Li, K. Beil, C. Kränkel and G. Huber, *Opt. Lett.*, 2012, **37**, 2568–2570.

7 C. Kränkel, J. Saraceno, O. H. Heckl, C. R. E. Baer, M. Golling, T. Südmeyer, K. Beil, K. Petermann, G. Huber and U. Keller, presented at the 2nd EOS Topcial Meeting Lasers, Capri, Italy, 2011, Talk 4559.

8 T. Jensen, A. Diening, G. Huber and B. H. T. Chai, *Opt. Lett.*, 1996, **21**, 585–587.

9 R. C. Pastor and A. C. Pastor, *Mater. Res. Bull.*, 1966, **1**, 275–282.

10 C. Chen, B. M. Wanklyn and P. Ramasamy, *J. Cryst. Growth*, 1990, **104**, 672–676.

11 D. B. Gasson and B. Cockayne, *J. Mater. Sci.*, 1970, **5**, 100–104.

12 B. M. Tissue, L. Lu, L. Ma, W. Jia, M. L. Norton and W. M. Yen, *J. Cryst. Growth*, 1991, **109**, 323–328.

13 C. McMillen, D. Thompson, T. Tritt and J. Kolis, *Cryst. Growth Des.*, 2011, **11**, 4386–4391.

14 C. McMillen and J. Kolis, *Philos. Mag.*, 2012, **92**, 2686–2711.

15 C. McMillen, L. Sanjeewa, C. Moore, D. Brown and J. Kolis, *J. Cryst. Growth*, 2016, **452**, 146–150.

16 M. Guzik, J. Pejchal, A. Yoshikawa, A. Ito, T. Goto, M. Siczek, T. Lis and G. Boulon, *Cryst. Growth Des.*, 2014, **14**, 3327–3334.

17 V. Peters, A. Bolz, K. Petermann and G. Huber, *J. Cryst. Growth*, 2002, **237–239**, 879–883.

18 L. Fornasiero, E. Mix, V. Peters, K. Petermann and G. Huber, *Cryst. Res. Technol.*, 1999, **34**, 255–260.

19 B. Mackintosh, A. Seidl, M. Ouellette, B. Bathey, D. Yates and J. Kalejs, *J. Cryst. Growth*, 2006, **287**, 428–432.

20 R. E. Novak, R. Metzl, A. Dreeben, S. Berkman and D. L. Patterson, *J. Cryst. Growth*, 1980, **50**, 143–150.

21 M. G. Hur, W. S. Yang, S. J. Suh, M. A. Ivanov, V. V. Kochurikhin and D. H. Yoon, *J. Cryst. Growth*, 2002, **237–239**(Part 1), 745–748.

22 T. F. Ciszek, *Mater. Res. Bull.*, 1972, **7**, 731–737.

23 W. Mu, Z. Jia, Y. Yin, Q. Hu, Y. Li, B. Wu, J. Zhang and X. Tao, *J. Alloys Compd.*, 2017, **714**, 453–458.

24 W. Mu, Y. Yin, Z. Jia, L. Wang, J. Sun, M. Wang, C. Tang, Q. Hu, Z. Gao, J. Zhang, N. Lin, S. Veronesi, Z. Wang, X. Zhao and X. Tao, *RSC Adv.*, 2017, **7**, 21815–21819.

25 W. Mu, Z. Jia, Y. Yin, B. Fu, J. Zhang, J. Zhang and X. Tao, *CrystEngComm*, 2019, **21**, 2762.

26 C. Guguschev, Z. Galazka, D. J. Kok, U. Juda, A. Kwasniewski and R. Uecker, *CrystEngComm*, 2015, **17**, 4662.

27 B. Fu, W. Mu, J. Zhang, X. Wang, W. Zhuang, Y. Yin, Z. Jia and X. Tao, *CrystEngComm*, 2020, **22**, 5060–5066.

28 M. F. Berard, C. D. Wirkus and D. R. Wilder, *J. Am. Ceram. Soc.*, 1968, **51**, 644.

29 L. Fornasiero, E. Mix, V. Peters, K. Petermann and G. Huber, *Ceram. Int.*, 2000, **26**, 589–592.

30 P. A. Loiko, K. V. Yumashev, R. Schödel, M. Peltz, C. Liebald, X. Mateos, B. Deppe and C. Kränkel, *Appl. Phys. B: Lasers Opt.*, 2015, **120**, 601–607.

31 K. Petermann, L. Fornasiero, E. Mix and V. Peters, *Opt. Mater.*, 2002, **19**, 67–71.

32 J. Burton, R. Prim and W. Slichter, *J. Chem. Phys.*, 1953, **21**, 1987.

33 R. Peters, C. Kränkel, K. Petermann and G. Huber, *J. Cryst. Growth*, 2008, **310**, 1934–1938.